

68815

Oriented Glassy Polymict Breccia

1789 grams



Figure 1: PET photo of 68815, outer surface eroded by zap pits. NASA# S72-37154. Cube is 1 cm.

Introduction

Sample 68815 was chipped off the top of a large (1 m) boulder and has a well known lunar orientation. The outer surface is covered with zap pits (figure 1) and the broken surface contains large vugs and vesicles (figure 2). 68815 is one of the samples that date the age of South Ray Crater (Drozd et al. 1974; Pepin et al. 1974) and is said to have had a simple exposure history.

68815 has been extensively studied as a “beam stop” for solar radiation and has been proposed as a “reference standard” for cosmic ray studies (Behrmann et al. 1973).

Petrography

68815 contains a variety of small (~1 mm) anorthositic clasts welded in a heterogeneous, glassy matrix (Brown

et al. 1973). The brown to yellow basaltic glasses are banded on a fine scale in complex swirl and lobate patterns. The unmelted fragments include gabbroic, noritic and troctolitic variants, but all are rich in plagioclase. No clasts equivalent of mare basalt are found.

Dixon and Papike (1978) describe two prominent lithic clasts in 68815 (figure 2). Clast I is composed of approximately 40% olivine and orthopyroxene, 60% plagioclase and small amounts of ilmenite, chrome spinel and Fe metal. Small, anhedral opx and olivine grains are dispersed throughout a feldspar matrix which is optically continuous over tens of millimeters. Clast II is 30% mafic, 70% plagioclase and has a poikiloblastic texture with orthopyroxene oikocrysts surrounding anorthite and olivine.

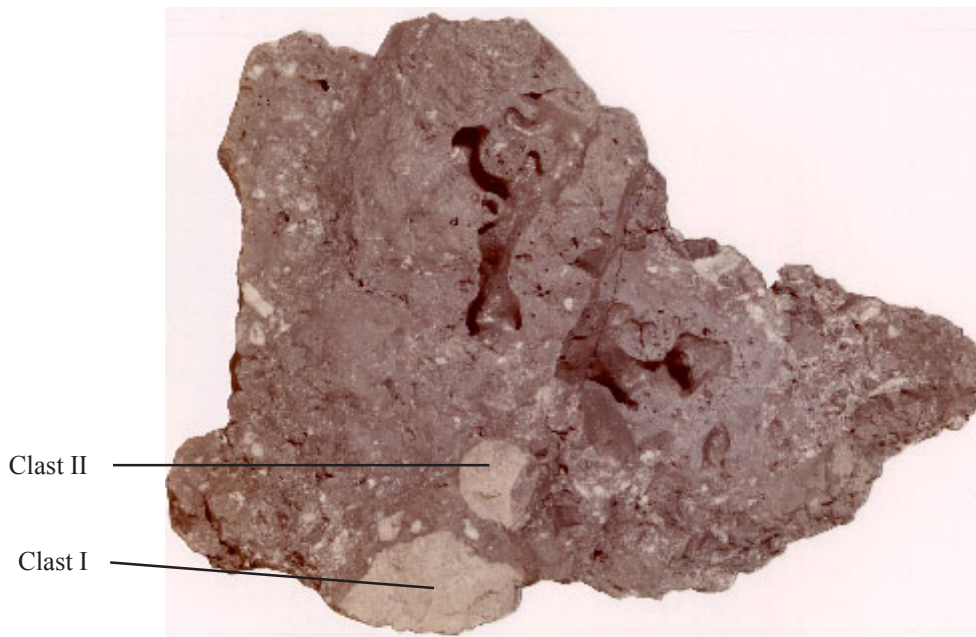


Figure 2: PET photo of 68815, freshly broken surface showing two rock clasts and large, elongate vesicles. NASA# S72-37155. Sample 14 cm across.

Mineralogy

Pyroxene: Dixon and Papike (1978) reported pyroxene compositions of lithic clasts in 68815 (figure 3).

Olivine: Olivine composition ranges Fo₆₉₋₇₃.

Plagioclase: Plagioclase ranges An₉₆₋₉₀.

Glass: Glass compositions are reported in Dixon and Papike (1978) (Al₂O₃ = 20-35%).

Metal grains were analyzed by Misra and Taylor (1975). Brown et al. (1973) give the analysis of shreibersite-iron intergrowth (with high Ni).

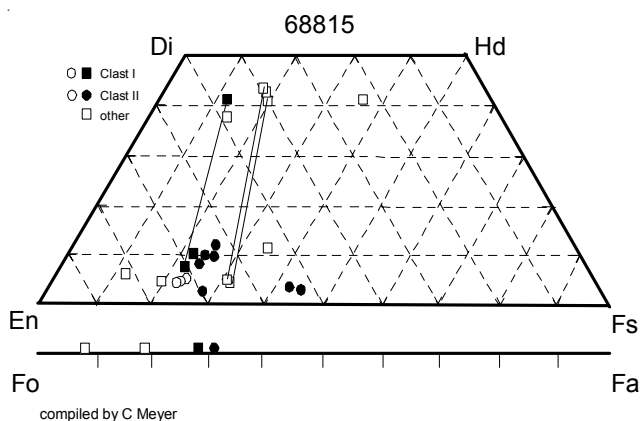


Figure 3: Olivine and pyroxene composition in 68815 (replotted from Dixon and Papike 1978).

Chemistry

68815 is heterogeneous by its nature (figure 2). Major elements were determined as part of the preliminary examination (LSPET 1973), by “classical methods” (Scoon 1974) and by Wänke et al. (1974)(table 1). Kohl et al. (1978) determined Fe, Al and Mn by atomic absorption in 14 different sub-samples and found rather consistent results (FeO = 3.14 – 5.5; Al₂O₃ = 26.5 – 30.5). Trace elements were determined by Krähenbühl et al. (1973), Wänke et al. (1974) and Fruchter et al. (1974) (figure 4).

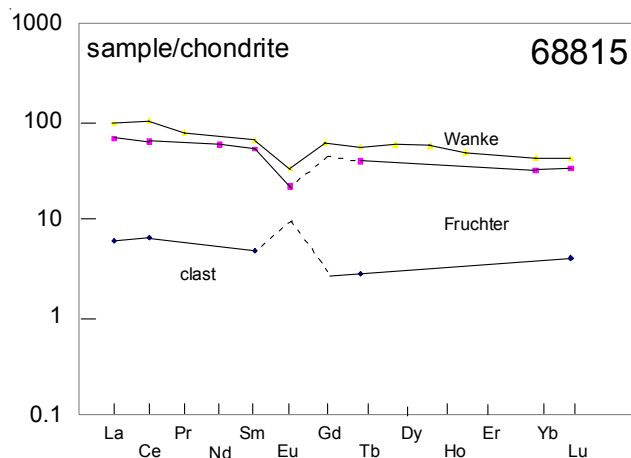


Figure 4: Normalized rare-earth-element diagram for matrix and clast in 68815 (data from Wanke et al. 1974, Fruchter et al. 1974).

Table 1. Chemical composition of 68815.

reference weight	Wanke 74	Scoon 74	Krahenbuhl 73	Clark 73 35 g	Fruchter et al. 74	LSPET 73	Kohl 78 14 sub-samples ranging from
SiO ₂ %	46.7	45.33 (b)				45.1 (e)	
TiO ₂	0.52	0.48 (b)				0.49 (e)	
Al ₂ O ₃	26.8	27.59 (b)				27.15 (e)	26.52 30.44 (f)
FeO	4.97	5.17 (b)			0.77 5.14 (a)	4.75 (e)	5.5 3.14 (f)
MnO	0.06	0.05 (b)				0.06 (e)	
MgO	6.38	5.38 (b)				5.88 (e)	
CaO	15	15.56 (b)				15.45 (e)	
Na ₂ O	0.53	0.48 (b)			0.42 0.5 (a)	0.42 (e)	
K ₂ O	0.22	0.17 (b)		0.15 (d)		0.14 (e)	
P ₂ O ₅		0.21 (b)				0.18 (e)	
S %		0.06 (b)				0.06 (e)	
sum		100.48				99.68	
Sc ppm	7.2 (a)				1.6 7.3 (a)		
V							
Cr	650 (a)				110 750 (a)	690 (e)	
Co	30.2 (a)				2.6 50.9 (a)		
Ni	500 (a)		360 (c)			206 (e)	
Cu	7.8 (a)						
Zn			2.54 (c)				
Ga	3.6 (a)						
Ge ppb	1.4 (a)		1.04 (c)				
As	0.74 (a)						
Se			0.107 (c)				
Rb	8.8 (a)		2 (c)			3.4 (e)	
Sr	160 (a)					175 (e)	
Y	64.4 (a)					61 (e)	
Zr	331 (a)					266 (e)	
Nb	20 (a)					16 (e)	
Mo							
Ru							
Rh							
Pd ppb	36 (a)						
Ag ppb			2.8 (c)				
Cd ppb			38 (c)				
In ppb							
Sn ppb							
Sb ppb			3.88 (c)				
Te ppb			5.2 (c)				
Cs ppm	460 (a)		125 (c)				
Ba	300 (a)				160 160 (a)		
La	22.3 (a)				1.4 15.4 (a)		
Ce	61 (a)				3.9 37 (a)		
Pr	6.8 (a)						
Nd						26 (a)	
Sm	9.4 (a)				0.7 7.6 (a)		
Eu	1.84 (a)					1.2 (a)	
Gd	11.9 (a)						
Tb	2 (a)				0.1 1.4 (a)		
Dy	14.1 (a)						
Ho	3.1 (a)						
Er	7.6 (a)						
Tm							
Yb	6.86 (a)					5.1 (a)	
Lu	1 (a)				0.1 0.8 (a)		
Hf	7.5 (a)				0.4 5.3 (a)		
Ta	0.93 (a)					0.5 (a)	
W ppb	0.45 (a)						
Re ppb			1.23 (c)				
Os ppb							
Ir ppb	11 (a)		11.8 (c)				
Pt ppb							
Au ppb	15 (a)		8.32 (c)				
Th ppm	3.74 (a)			2.74 (d)	0.3 2.8 (a)	3.7 (e)	
U ppm	1.09 (a)		0.57 (c)	0.81 (d)			

technique (a) INAA, (b) classical wet grav., (c) RNAA, (d) counting, (e) XRF, (f) AA.

Chemical data for the two prominent white clasts (figure 2) appear to be lacking.

Radiogenic age dating

Schaeffer et al. (1976) and Schaeffer and Schaeffer (1977) reported $^{39}\text{Ar}/^{40}\text{Ar}$ plateau and K/Ar ages for glass and several clasts within 68815 (figures 5-6).

Cosmogenic isotopes and exposure ages

Behrmann et al. (1973) and Drozd et al. (1974) determined the cosmic ray exposure age of 68815 (2.04 ± 0.08 m.y.) by the ^{81}Kr -Kr method and associated this age with the South Ray Crater event.

This rock provided an ideal substrate to study the interaction of solar cosmic rays. Clark and Kieth (1973) determined the activity of ^{22}Na (56 ± 11 dpm/kg), ^{26}Al (150 ± 30 dpm/kg), ^{53}Mn (21 ± 6 dpm/kg), ^{56}Co and ^{46}Sc for a bulk sample (34.5 g) of 68815. Fruchter et al. (1977, 1978) determined ^{26}Al (63 ± 2.4 dpm/kg) and ^{53}Mn (71 ± 6 dpm/kg). Kohl et al. (1978) determined

the depth profiles for ^{53}Mn (265 to 83 dpm/kg)(figure 7) and ^{26}Al (337 to 96 dpm/kg)(figure 8). Jull et al. (1998) determined the ^{14}C depth profile (figure 9). Rao et al. (1994) determined depth profiles for ^3He , ^{21}Ne and ^{38}Ar (figure 10). Nishiizumi et al. (1988) determined ^{10}Be and found that it did not vary as a function of depth.

The depth profile studies of ^{14}C by Jull et al. (1998) showed that the radiation hardness (rigidity R_0) and flux of solar protons was higher than that determined by ^{10}Be , ^{26}Al and ^{53}Mn measurements.

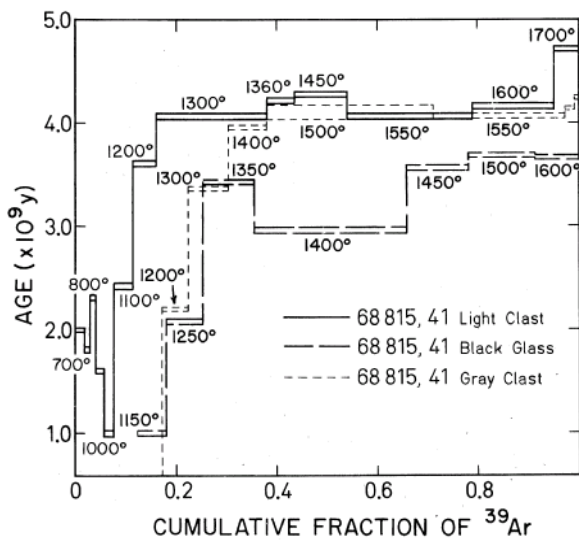


Figure 5: Argon release diagrams for $^{39}\text{Ar}/^{40}\text{Ar}$ age dating plateau (from Schaeffer et al. 1976).

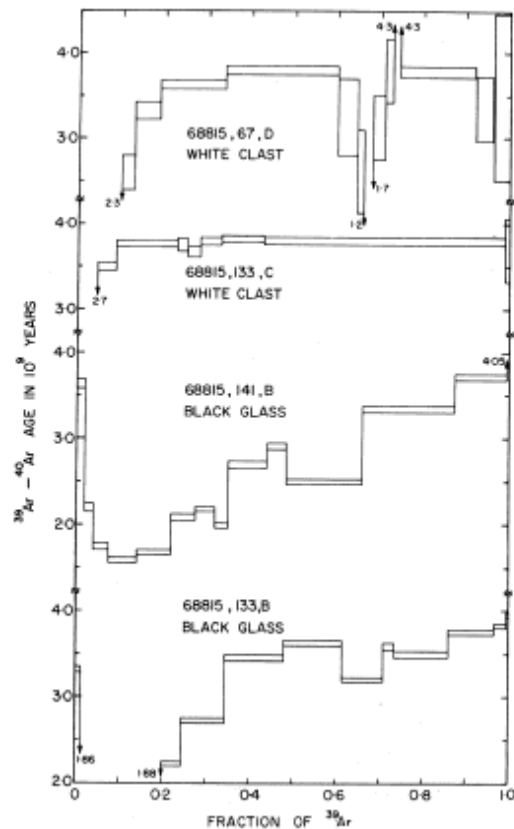


Figure 6: Argon release data for age dating by Schaeffer and Schaeffer (1977).

Summary of Ages

	K ppm	Ar Plateau	K/Ar	reference
Glass	1458		2.681 ± 0.003	Schaeffer x2 (1977)
Glass	1646		3.015 ± 0.003	Schaeffer x2 (1977)
Clast	489	3.811 ± 0.012	3.686 ± 0.007	Schaeffer x2 (1977)
Clast	214		3.54 ± 0.02	Schaeffer x2 (1977)
Clast II	700	4.120 ± 0.04	4.01 ± 0.01	Schaeffer et al. (1976)
Clast	1153	4.02 ± 0.024	3.66 ± 0.04	Schaeffer et al. (1976)
Glass	1156	3.63 ± 0.054	3.05 ± 0.01	Schaeffer et al. (1976)
Glass	1602	3.692 ± 0.037	3.3 ± 0.01	Schaeffer et al. (1976)
Clast I	289	4.073 ± 0.027	3.76 ± 0.01	Schaeffer et al. (1976)

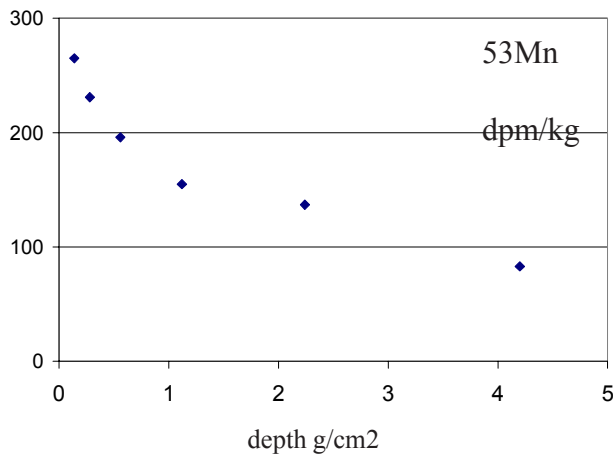


Figure 8: Mn 53 depth profile for 68815 from Kohl et al. (1978).

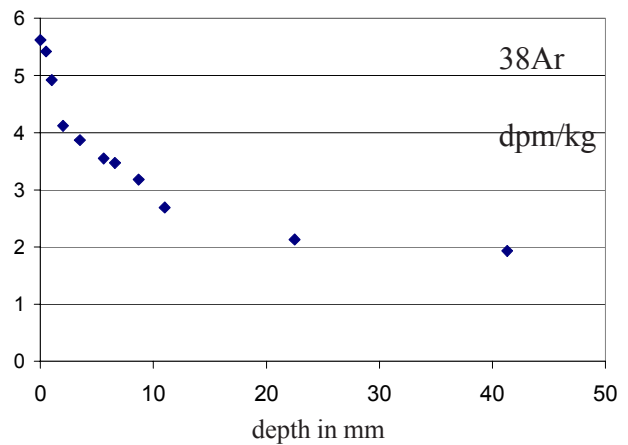


Figure 10: Ar 38 depth profile in 68815 from Rao et al. (1994).

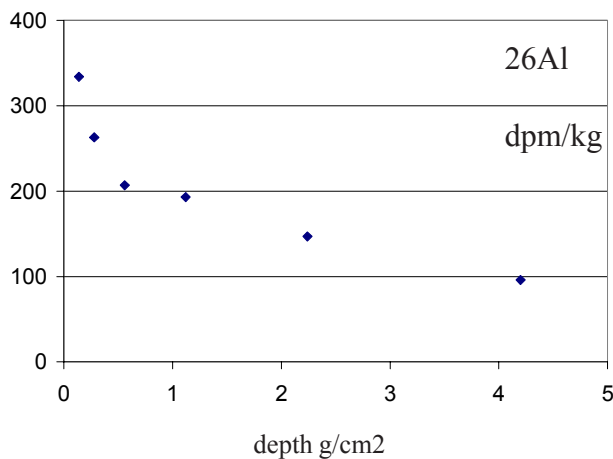


Figure 7: Al 26 depth profile for 68815 from Kohl et al. (1978).

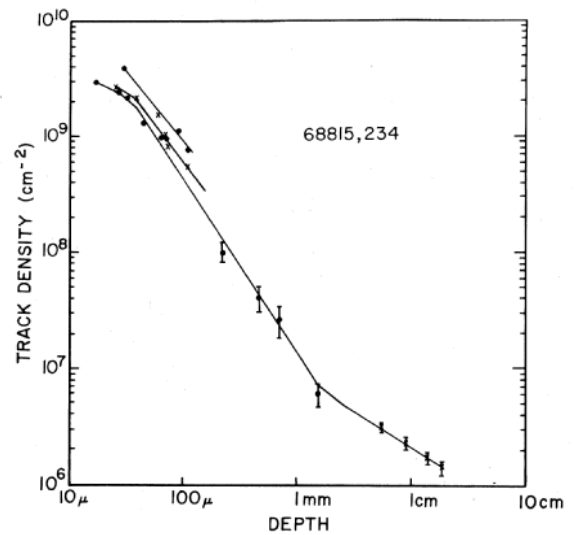


Figure 11: Nuclear tracks recorded in 68815 (from Dust and Crozaz 1977).

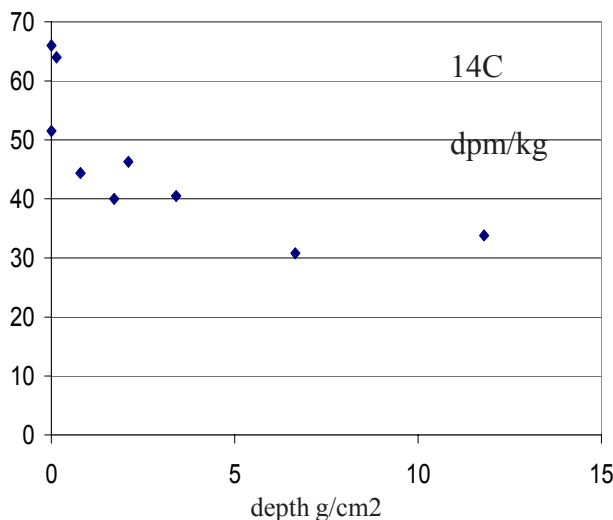


Figure 9: C 14 depth profile for 68815 from Jull et al. (1998).

Jull et al. (1995) detected a small amount of solar-implanted ¹⁴C in etched samples of patina scrapped from the surface of 68815, although less than predicted by Fireman et al. (1977).

Other Studies

Sample 68815 was proposed initially as a “reference standard” for cosmic ray track and micrometeorite density studies (Behrmann et al. 1973), because of its simple exposure history. Behrmann et al. (1973) counted between 30 and 50 pits > 30 micron in size on a ½ cm² surface area, which is about 4 times higher than what was predicted by Morrison et al (1973). Walker and Yuhas (1973) and Dust and Crozaz (1977) determined nuclear track density as a function of depth (figure 11). The density of tracks is found to be

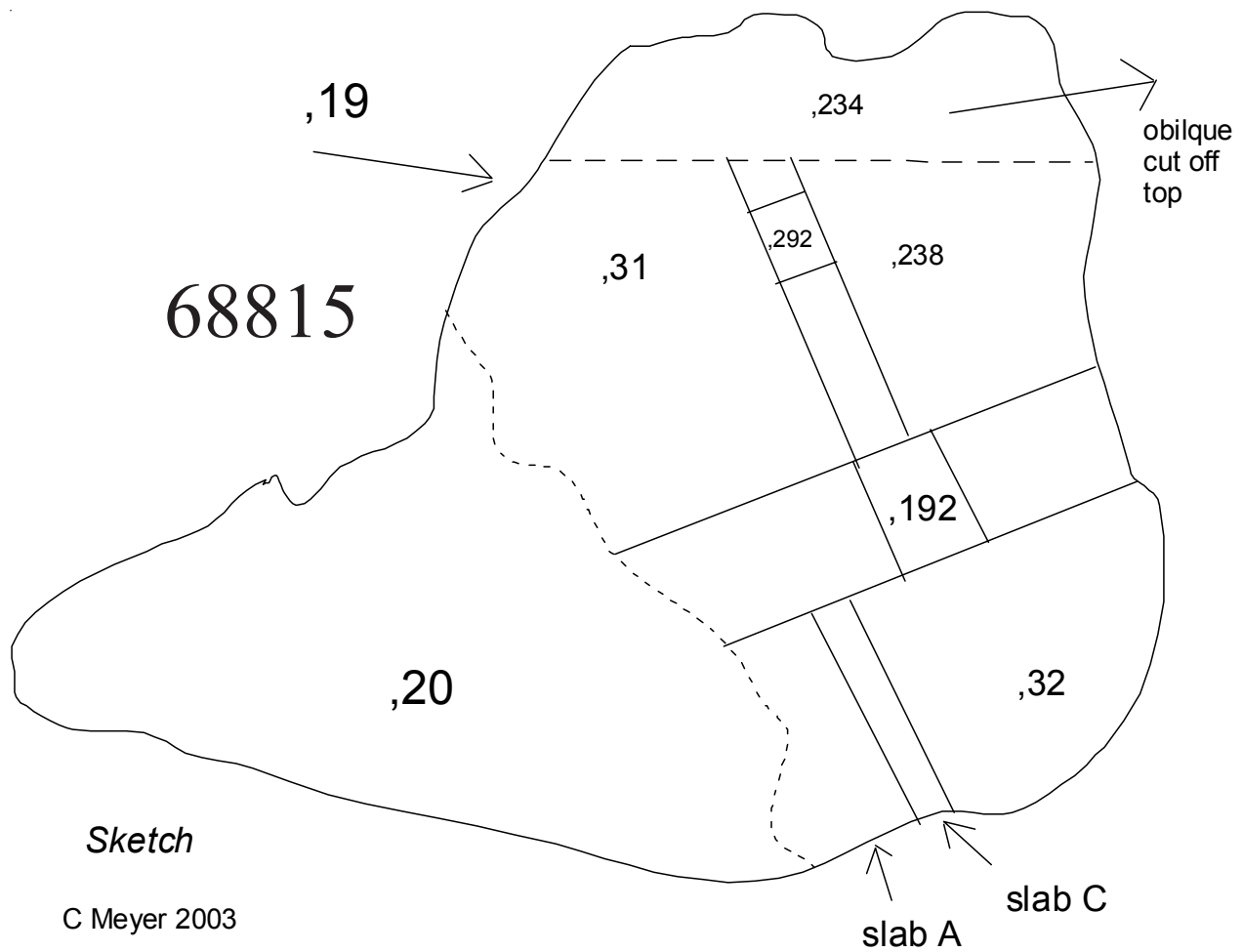


Figure 12: Sketch of 68815 showing approximate location of initial break (,19,20), saw cuts to produce slabs and columns and top piece for radiation studies. Sketch prepared by C Meyer (see figure 1 for reference).



Figure 13: Group photo of saw cuts to produce column 68815,192 and ,191. NASA # S74-27981.

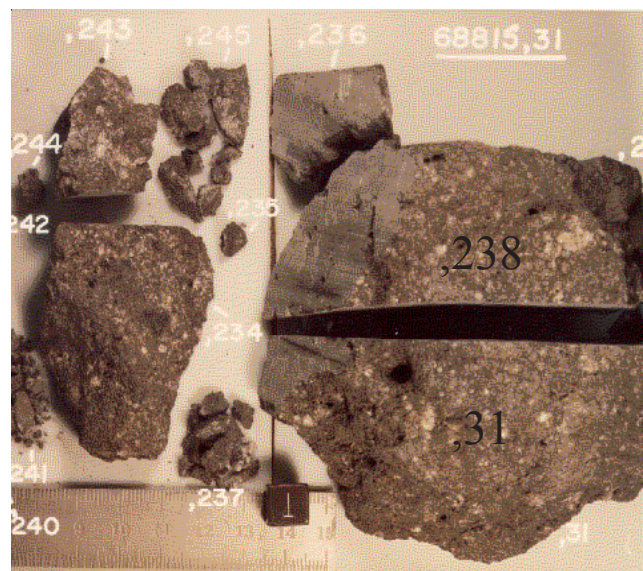


Figure 14: Group photo of processing for slab ,238 and top piece ,234 of 68815. NASA # S75-33561.

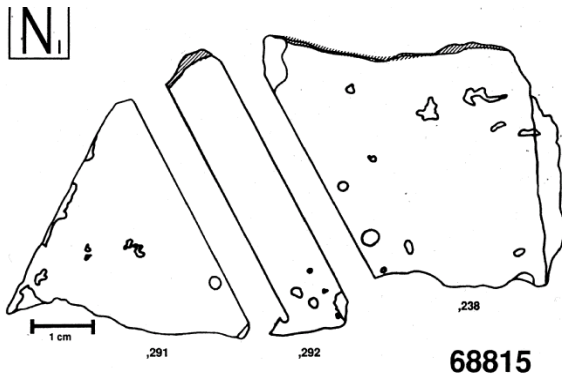


Figure 15: Slab 68815,238 (from Jull et al. 1998).

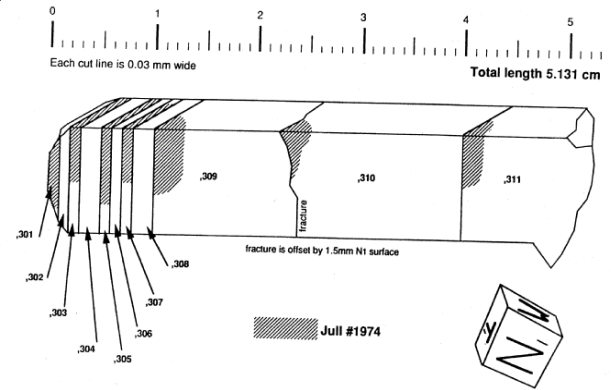


Figure 16: Column 68815,292 used for ¹⁴C depth profile (figure from Jull et al. 1998).

consistent with the 2 m.y. exposure history and erosion rate of 1-2 mm per m.y. Dust and Crozaz go on to claim that *“the agreement of this spectrum with that measured for contemporary cosmic rays demonstrates the long term-constancy of the galactic cosmic ray flux of very heavy ions”* (one wonders).

Leich et al. (1973, 1974), Padawer et al. (1974) and Stauber et al. (1973) studied the H and F content of the surface of 68815 and Goldberg et al. (1976) studied vesicle walls.

Nagata et al. (1973), Cisowski et al, (1974) and Schwrer and Nagata (1976) studied magnetic properties of 68815. Schwerer et al. (1973), Huffman et al. (1974) and Huffman and Dunmyre (1975) reported Mossbauer spectra.

Processing

In 1972, 68815 broke into two pieces (labeled ,19 and ,20 see sketch, figure 12) and sub-sample ,19 was sawn into ,32 and ,31. Sub-sample ,32 was sawn into slabs A and C. In 1974, sub-sample ,31 was divided by sawing to obtain a thick (1 in) column (top ,192; bottom ,191)(figure 13). In 1975, the remainder of ,31 was sawn on an oblique angle to obtain a top piece (,234; figure 14), and in half to produce ,238 and ,31 (now smaller). In 1992-3, ,238 was sawn again to obtain a slab and a column ,292 (as perpendicular to the lunar surface as could be obtained)(sketches figures 15-16).

List of Photos #s for processing of 68815.

- S72-37152-37156 PET, Color
- S72-41425 Orientation and lighting
- S72-40984-40999 PET B&W
- S72-48079-48083 First break ,19 ,20
- S72-48959-48960 Group photo
- S74-27977-27982 Group photo, subdivision ,31
- S75-33396 Group
- S75-33421 split ,238
- S75-33427-33433
- S91-30264-30268
- S92-32816 Outer surface
- S92-32823 Zap pits